Hyperspectral Remote Sensing and Plant

Subjects: Plant Sciences | Agricultural Engineering | Remote Sensing
Contributor: Alexander Fedotov

Hyperspectral remote sensing provides image data with very high spectral resolution. This high resolution allows subtle differences in plant health to be recognized. Such a multidimensional data space, generated by hyperspectral sensors, has given rise to new approaches and methods for analyzing hyperspectral data.

Keywords: remote sensing ; hyperspectral ; plant diseases ; early detection ; oil palm ; citrus ; cereals ; solanaceae

1. Introduction

The spread of various, including invasive, plant diseases and pests is one of the most important problems in modern agriculture [1]. Therefore, to solve these relevant problems, the timely monitoring of plant diseases and pests is necessary. Remote sensing methods hold great promise for solving these problems [2]. Remote sensing data can identify crop conditions, including diseases, and provide useful information for specific agricultural management practices [3][4].

There are two types of remote sensing technologies: passive (such as optical) and active remote sensing (such as LiDAR and radar). Passive optical remote sensing is usually divided into two groups based on the spectral resolution of the sensors used: multispectral and hyperspectral remote sensing [5]. Hyperspectral sensing shows great potential as a non-invasive and non-destructive tool for monitoring biotic and abiotic plant stress among passive remote sensing methods, which measure reflected solar radiation [6]. This method collects and stores information from the spectroscopy of an object in a spectral cube that contains spatial information and hundreds of contiguous wavelengths in the third dimension. Hyperspectral imaging offers many opportunities for the early recognition of plant diseases by providing preliminary indicators through subtle changes in spectral reflectance due to absorption or reflection. Hyperspectral images with hundreds of spectral bands can provide detailed spectral portraits, hence, they are better able to detect subtle variations in soil, canopies or individual leaves. Thus, hyperspectral images can be used to solve a wider class of problems for the accurate and timely determination of the physiological status of agricultural crops. The early identification of disease spread and pest outbreaks may avoid not only significant crop loss, but also reduce pesticides usage and mitigate their negative impacts on human health and the environment, thus, improving the existing IPM [7][8].

In recent years, a wide range of miniature hyperspectral sensors available for commercial use have been developed, such as Micro- and Nano-Hyperspec (Headwall Photonics Inc., Boston, MA, USA), HySpex VNIR (HySpex, Skedsmo, Skjetten, Norway) and FireflEYE (Cubert GmbH, Ulm, Germany) [9]. These sensors can be installed on manned or unmanned airborne platforms (for example, airplanes, helicopters, and UAVs) to obtain hyperspectral imaging and support various monitoring missions [10][11].

There are various types of hyperspectral cameras, e.g., push-broom cameras, whisk-broom cameras and snapshot cameras. The measurement principle of each sensor type depends on its ability to obtain the whole picture (snapshot) at one time, one line of the picture (push broom) or one point of the picture (whisk broom) [12].

The general routine of collecting and processing hyperspectral images is presented in **Figure 1**. The light reflected from plant leaves is collected by the hyperspectral camera (**Figure 1**A) [13]. A hyperspectral data cube (**Figure 1**B) is obtained from the hyperspectral camera. Then various data normalization (**Figure 1**C) and feature extraction (**Figure 1**D) algorithms are applied to reduce the data's dimensionality. Finally, different automatization techniques are used to automate the classification process (**Figure 1**E).

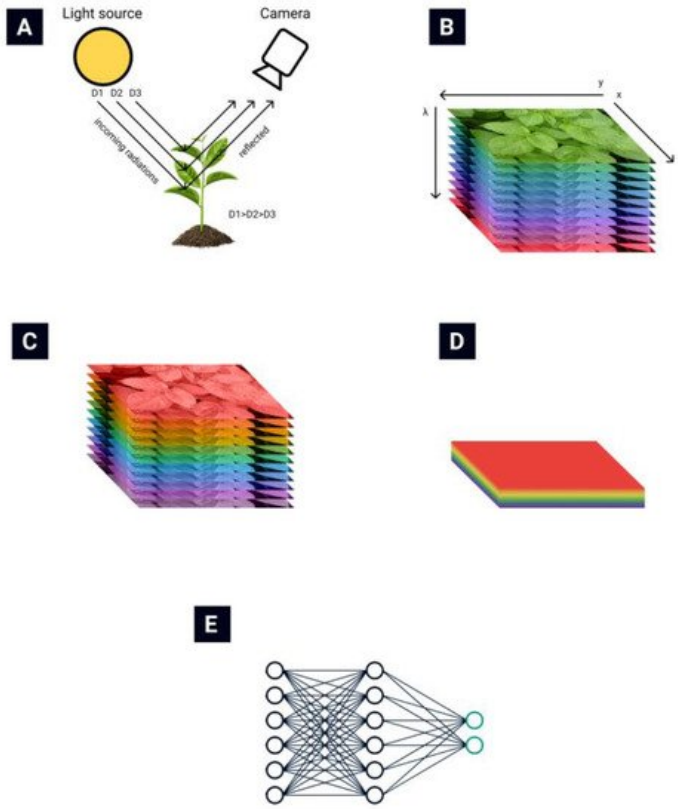

Figure 1. Hyperspectral data retrieval and processing (remastered from [14][15]). (**A**) Reflected light collection by the hyperspectral camera, (**B**) a hyperspectral data cube, (**C**) data normalization, (**D**) feature extraction, (**E**) automation of the classification process.

Hyperspectral remote sensing provides image data with very high spectral resolution [16][17]. This high resolution allows subtle differences in plant health to be recognized. Such a multidimensional data space, generated by hyperspectral sensors, has given rise to new approaches and methods for analyzing hyperspectral data [18][19].

For a long time, feature extraction methods have been used that reduce the data dimension without loss (or with minimal loss) of the original information on which the classification of hyperspectral images is based [20]. One of the most widely used dimensionality reduction techniques in HRS is principal component analysis (PCA). PCA computes orthogonal projections that maximize data variance and outputs the dataset in a new, uncorrelated coordinate system. Unfortunately, the informational content of hyperspectral images does not always coincide with such projections [21]. Thus, other methods are also used for feature extraction. The common methods for extracting hyperspectral data used in pathological research traditionally include PCA [22], derivative analysis [23], wavelet methods and correlation plots [24]. Alternatively, the hyperspectral image data can be processed at the image level to extract either spatial representation alone or joint spatial spectral information. If only spatial features are considered, for example, when studying structural and morphological features, spatial patterns among neighboring pixels with relation to the current pixel in the hyperspectral image will be extracted. Machine vision techniques, such as using a two-dimensional CNN, with a $p \times p$ chunk of input pixel data have been implemented to automatically generate high-level spatial structures. Extraction of spatial characteristics, in tandem with spectral elements, has been shown to significantly improve model performance. [25]. The use of spatial spectral characteristics can be achieved using two approaches: (i) by separately extracting spatial characteristics using CNN [26][27] and combining data from a spectral extractor using RNN, or LSTM [27][28]; and (ii) by using three-dimensional patterns in hyperspectral data cubes ($p \times p \times$ b) associated with $p \times p$ spatially adjacent pixels and b spectral bands to take full advantage of important distinctive patterns.

2. Hyperspectral Remote Sensing for Early Plant Disease Detection

It was believed that, due to the lack of interaction between specialists in engineering and biology, there is a significant gap in the scientific basis for planning an experiment to use remote sensing data in determining plant state. Although the above demonstrates the practical possibility of late and early detection of plant diseases using HRS, it also reveals differences in the technical results (range of important bands) between researchers, which indicates an insufficient study of the experimental methodology, as can be seen from **Table 1**, **Table 2**, **Table 3** and **Table 4**.

Table 1. Oil palm disease early detection by HRS.

Publication Year	Culture	Treat	Equipment	Studied Bands	Important Bands	Study Type	Reference	Location
2009	oil palm	basal stem rot	APOGEE spectroradiometer of unmentioned model	450–1100	715, 734, 791	field	[29]	Malaysia
2009	oil palm	basal stem rot	APOGEE spectroradiometer of unmentioned model	300–1000	462, 487, 610.5, 738, 749	field	[30]	Malaysia
2010	oil palm	basal stem rot	PP Systems Unispec-SC spectrometer	310–1130	670–715, 490–520, 730–770, 920–970	field	[31][32]	Indonesia
2011	oil palm	basal stem rot	APOGEE spectroradiometer of unmentioned model	350–1000	495, 495.5, 496, 651.5, 652, 652.5, 653, 653.5, 654, 654.5, 655, 655.5, 656, 656.5, 657, 657.5, 658, 658.5, 659, 659.5, 660, 660.5, 661, 908	field	[33]	Malaysia
2014	oil palm	basal stem rot	ASD spectrometer of unmentioned model	325–1040	not mentioned	field	[34]	Malaysia
2017	oil palm	basal stem rot	APOGEE spectroradiometer of unmentioned model	325–1000	495, 495.5, 496, 651.5, 652, 652.5, 653, 653.5, 654, 654.5, 655, 655.5, 656, 656.5, 657, 657.5, 658, 658.5, 659, 659.5, 660, 660.5, 661, 908	field	[35]	Malaysia
2017	oil palm	basal stem rot	GER 1500 spectrometer	273–1100	540–560, 650–780	field	[36]	Malaysia
2018	oil palm	basal stem rot	Specim spectrograph of unmentioned model	350–1000	650–750	field	[37]	Malaysia
2020	oil palm	basal stem rot	Cubert S185 camera	325–1075	800–950	greenhouse	[38]	Malaysia
2014	oil palm	orange spotting	ASD FieldSpec 4 spectrometer	300–1050	400–401, 404–405, 455–499, 500–599, 600–699, 700–712	field	[39][40]	Malaysia
2019	oil palm	orange spotting	ASD HandHeld 2 spectrometer	400–1050	601–630	field	[41]	Malaysia
2019	oil palm	orange spotting	ASD HandHeld 2 spectrometer	325–1075	680–780	field	[42][43]	Malaysia

Table 2. Citrus disease early detection by HRS.

Publication Year	Culture	Treat	Equipment	Studied Bands	Important Bands	Study Type	Reference	Location
2012	citrus	citrus greening	Spectra Vista SVC HR-1024 spectrometer	350–2500	537, 612, 638, 662, 688, 713, 763, 813, 998, 1066, 1120, 1148, 1296, 1445, 1472, 1546, 1597, 1622, 1746, 1898, 2121, 2172, 2348, 2471, 2493	field	[44][45][46]	USA
2012	citrus (orange)	citrus greening	Spectra Vista SVC HR-1024 spectrometer & Varian Cary 500 Scan	457–921	650–850	field and lab	[47]	USA
2012	citrus (orange)	citrus greening	Specim Aisa Eagle camera	457–921	410–432, 440–509, 634–686, 734–927, 932, 951, 975, 980	field	[48]	USA
2018	citrus	citrus greening	Specim Imspector V10E spectrograph combined with camera	379–1023	493, 515, 665, 716, 739	lab	[49]	China
2019	citrus	citrus greening	Cubert S185 camera and ASD HandHeld 2 spectrometer	400–1000	544, 718, 753, 760, 764, 930, 938, 943, 951, 969, 985, 998, 999	field	[50]	China
2020	citrus	citrus greening	Cubert S185 camera & ASD HandHeld 2 spectrometer	450–950, 325–1075	468, 504, 512, 516, 528, 536, 632, 680, 688, 852	field	[51]	China
2020	citrus	citrus greening	ASD HandHeld 2 spectrometer	370–1000	not mentioned	field	[52]	China

Table 3. *Solanaceae* disease early detection by HRS.

Publication Year	Culture	Treat	Equipment	Studied Bands	Important Bands	Study Type	Reference	Location
2003	tomato	late blight	Megatech GER-2600 spectrometer	400–2500	750–930, 950–1030, 1040–1130	field	[53]	USA
2014	tobacco	TSWV	Ocean Optics USB2000 spectrometer	450–850	475.22, 489.37, 524.29, 539.65, 552.82, 667.33, 703.56, 719.31, 724.31, 758.39	greenhouse	[54]	Bulgaria
2015	tomato	late blight, early blight	Specim Imspector V10E spectrograph combined with camera	400–1000	442, 508, 573, 696, 715	lab	[55]	China
2017	tomato	gray mold	Specim Imspector V10E spectrograph combined with camera	380–1023	655, 746, 759–761	lab	[56]	China

Publication Year	Culture	Treat	Equipment	Studied Bands	Important Bands	Study Type	Reference	Location
2017	tomato	yellow leaf curl	Specim Imspector V10E spectrograph combined with camera	450–1000	560–575, 712–729, 750–950	lab	[57]	China
2017	tobacco	TMV	Specim Imspector V10E spectrograph combined with camera	450–1000	697.44, 639.04, 938.22, 719.15, 749.90, 874.91, 459.58, 971.78	lab, greenhouse	[58][59]	China
2018	tomato	late blight, target and bacterial spot	Spectra Vista SVC HR-1024 spectrometer	350–2500	445, 450, 690, 707, 750, 800, 1070, 1200	lab	[60]	USA
2018	tomato	TSWV	Specim Imspector V10E spectrograph combined with camera	400–1000	700–1000	lab	[61]	Israel
2018	potato	PVY	ASD FieldSpec 4 spectrometer	350–2500	500–900, 720–1300	field	[62]	USA
2019	tomato	late blight, blackleg	StellarNet Blue Wave spectrometer	400–1000	not mentioned	greenhouse, field	[63]	UK
2019	tobacco	TSWV	Surface optics SOC710VP camera	400–1000	780–1000	lab	[64]	China
2019	potato	PVY	Specim FX10 camera	400–1000	not mentioned	field	[65]	The Netherlands
2019	potato	early blight	Specim Imspector V10E spectrograph combined with camera	430–900	550, 680, 720–750	field	[66]	Belgium
2019	tomato	bacterial spot, target spot	Resonon Pika L camera	380–1020	408–420, 630–650, 730–750	lab and field	[67]	USA
2019	pepper early	TSWV	Specim Imspector V10E spectrograph combined with a camera	400–1000	700–1000	lab	[68]	Israel
2019	potato	late blight	Senop Oy Rikola camera	500–900	620, 724, 803	field	[69]	The Netherlands
2020	tomato	yellow leaf curl, bacterial spot	Resonon Pika L camera	380–1020	550–850	lab and field	[67]	USA

Publication Year	Culture	Treat	Equipment	Studied Bands	Important Bands	Study Type	Reference	Location
2020	tomato early	ToCV	PP Systems Unispec-SC spectrometer	310–1100	402.2, 405.5, 412.2, 415.6, 425.7, 429.0, 449.2, 556.4, 559.7, 563.0, 566.4, 676.4, 679.7, 722.9, 726.3, 862.1	lab	[70]	Greece
2020	potato	late blight	ASD FieldSpec 4 spectrometer	400–900	439–481, 554–559, 654–671, 702–709	lab	[71]	Canada
2020	potato	late blight	ASD FieldSpec 4 spectrometer	660–780	668, 705, 717, 740	lab	[72]	Canada
2020	potato early	late blight, early blight	Spectra Vista SVC HR-1024 spectrometer	350–2500	700, 857, 970, 990, 1100, 1241, 1380, 1890, 2300	lab	[73][74]	USA

Table 4. Wheat disease early detection by HRS.

Publication Year	Culture	Treat	Equipment	Studied Bands	Important Bands	Study Type	Reference	Location
2000	wheat	fusarium	Specim Imspector V9 spectrometer combined with camera	425–860	not mentioned	lab	[75]	USA
2011	wheat	fusarium	Specim Imspector V10E spectrograph combined with camera	400–1000	500–533, 560–675, 682–733	lab and field	[76]	Germany
2015	wheat	fusarium	Headwall Photonics Hyperspec Model 1003B-10151 spectrometer combined with a camera	520–1785	1411	lab	[77]	Brazil
2018	wheat	fusarium	Specim Imspector V10E and ImSpector N25E spectrographs	400–1000, 1000–2500	430–525, 560–710, 1115–2500	greenhouse	[78][79]	Germany
2018	wheat	fusarium, yellow rust	Gilden Photonics camera	400–1000	650–700	lab, field	[80][81]	UK
2019	wheat	fusarium	ASD FieldSpec Pro spectrometer	350–2500	471, 696, 841, 963, 1069, 2272	field	[82]	China
2019	wheat	fusarium	Surface optics SOC710VP camera	400–1000	447, 539, 668, 673	field	[83]	China
2020	wheat	fusarium	Surface optics SOC710VP camera	400–1000	560, 565, 570, 661, 663, 678	field	[84]	China
2020	wheat	fusarium	ASD FieldSpec Pro spectrometer	350–2500	350–400, 500–600, 720–1000	field	[24]	China
2007	wheat	yellow rust	ASD FieldSpec Pro spectrometer	350–2500	not mentioned	field	[85]	China
2012	wheat	yellow rust	ASD FieldSpec Pro spectrometer	350–2500	not mentioned	field	[86]	China

Publication Year	Culture	Treat	Equipment	Studied Bands	Important Bands	Study Type	Reference	Location
2014	wheat	yellow rust	ASD FieldSpec Pro spectrometer	350–2500	428, 672, 1399	field	[87]	India
2019	wheat	yellow rust	ASD FieldSpec Pro spectrometer	350–1000	460–720, 568–709, 725–1000	field	[88]	China
2019	wheat	yellow rust	Specim ImSpector PFD V10E camera, Senop Oy Rikola camera	400–1000, 500–900	594, 601, 706, 780, 797, 874, 881	field	[89][90]	Germany
2019	wheat	yellow rust	Cubert S185 camera	450–950	not mentioned	field	[91]	China
2019	wheat	yellow rust	Headwall Photonics VNIR imaging sensor, Cubert S185 camera	400–1000	538, 598, 689, 702, 751, 895	lab, field	[92][93]	China

As a result of hyperspectral remote sensing, for each pixel of a scene, a random vector was got, which can be considered the result of a random experiment. The outcome of a random experiment can be favorable or unfavorable, which is associated with the detection or non-detection of a disease in the space reflected by a particular pixel. Accordingly, these vectors can be processed by methods developed in the theory of probability and in mathematical statistics, which make it possible to effectively determine the characteristics of a random experiment. In this case, the tasks of data normalization and the allocation of those frequency bands (important bands) that make the greatest contribution to the outcomes of experiments (favorable or unfavorable) and, accordingly, are the most informative for identifying diseases, can be solved. The selection of important bands is a critical step in the detection of plant diseases using HRS. As a rule, data normalization is carried out first to get rid of noise. Then, various algorithms are applied to identify important bands, such as Savitzky–Golay filtering [31][32][34][94][95][52][71][72][70][80][81][90]; the Mann–Whitney U test [29][96]; coefficient of variation [38]; PCA [45][47][51][60][66][71][70][76]; SPA [49][55][64][58][59][92]; GA and BRT [64]; SAM [73][74][83][89].

The listed algorithms make it possible to achieve the determination of important bands. Various methods of machine learning allow achieving a fairly high accuracy in identifying diseases (between 60 and 95% accuracy) based on those data. However, from **Table 1**, **Table 2**, **Table 3** and **Table 4**, it can be concluded that even under very similar experimental conditions—For example when studying oil palms—Different sets of important bands are obtained at the output, often with a spread of more than 100 nm [29][30][96][33][35][37][34][36][38]. Xie et al., in [56], used five different algorithms to select important bands, taken from five different studies: *t*-test [97], Kullback–Leibler divergence [98], Chernoff bound [99], receiver operating characteristics [100] and the Wilcoxon test [101]. It is noteworthy that, in 4 tests out of 5, only 1 frequency out of 15 matched closely. In this case, the scatter of the ranges of all initially selected important bands was in the range from 400 to 850 nm, (400, 402, 403, 411, 413, 418, 419, 420, 422, 473, 642, 690, 722, 756 and 850 nm), i.e., practically in the entire range of the used sensor (380–1020 nm).

It was assume that, in the experiments on the same section of a field, repeated in different years or seasons, different important bands will likely be allocated when using automatic selection methods. Unfortunately, at the moment it is not possible to test this theory, since there are very few articles in which such experiments would be described.

Summarizing the topic of choosing the important bands for plant disease detection, we assume that it would be logical to focus on studying the bands of biochemical changes occurring in diseased plants and screening out the bands not related to the given disease, rather than using machine learning.

To successfully conduct the biological component of experiments on the HRS of plant diseases, it is necessary to understand that plant diseases are a particular case of plant stress. Plant diseases are processes that occur in plants under the influences of various reasons and which lead to their oppression and decreased productivity. Plant diseases are divided into two main groups: infectious and non-infectious [102][103]. The infectious plant diseases are caused by microorganisms (mainly fungi, bacteria, viruses and nematodes) or parasitic plants. The non-infectious diseases can be caused by genetic disorders or physiological metabolic disorders resulting from unfavorable environmental conditions [102][103]. Plant diseases almost always have visible symptoms that can be observed in a certain spectral range. In their early stages, such symptoms appear in the form of various chloroses or, less often, necrosis or pustules, with a huge variety of manifestations [104][105]. In the case of an asymptomatic course of the disease in its early stages, for example barley Ramularia disease caused by *Ramularia collo-cygni* [106], Fusarium head blight of different cereals caused by *Fusarium*

culmorum [76] or soybean Sudden death caused by *Fusarium virguliforme* [107], early detection by remote sensing can be challenging.

Plant stress is a state of the plant in which it is influenced by unfavorable abiotic (light, heat, air, humidity, soil composition and relief conditions) and biotic factors (phytogenic, zoogenic, microbogenic and mycogenic). Plant responses to both abiotic and biotic stress is usually complex and includes both nonspecific (common for different stressors) and specific components. In a state of stress plants stop their growth, sharply reduce the activity of their root systems and reduce the intensity of photosynthesis and protein synthesis [108][109][110]. In a significant number of stressful situations, an immune response causes an increase of certain metabolites content, such as jasmonates or salicylates [110][111][112][113][114][115]. These reactions can be detected using hyperspectral sensors [116][117][118][119][120][121][122][123]. The study of plant stress using hyperspectral sensors is presented in a number of works [124][125][126], including those comparing the spectral portraits of plants simultaneously exposed to biotic and abiotic stress [127][128][129][130]. It is necessary to take into account many abiotic factors in addition to the possible influence of pathogens to accurately determine the reasons for stress manifestation [36][38][39][44][49][60][53][73][74][75][78][79][76][86]. The analysis indicates that there is no unified methodology for conducting hyperspectral studies of plant diseases that takes into account the influence of abiotic factors. That is why it is best to carry out experiments in laboratory conditions or in industrial greenhouses in order to partially or completely eliminate abiotic factors. Attempts to create various mobile vehicles operating at ground level whose purpose is to replace natural light sources with artificial light when using hyperspectral sensors in field experiments are described in [44][45][46][60][62][131]. This solves one of the main problems associated with the inhomogeneity of the solar spectrum due to changing weather conditions. Nevertheless, this approach cannot completely solve the problem of the influence of abiotic factors.

It would also be interesting to continue studies describing the definition of the phenotype and/or genotype of a plant and its influence on changes in the spectral portrait thereof [132][133][134][135][136][137]. Several studies reviewed describe that the host plant genotype has a significant impact on spectral reflectance and on the biochemical and physiological traits of the plants undergoing pathogen infection [47][49][63][69][73][74][75][78][79][85][86][90][88]. Therefore, it is very important to indicate the culture and cultivar of the studied plants. The exact indication of pathogens used for inoculation is also very important. It was believed that comparisons of the spectral portraits of plants of different cultivars of the same crop is a primary task in creating a general methodology for detecting plant diseases using hyperspectral sensors. It is possible that the influence of chlorophyll fluorescence on the spectral portraits of plants and their related SVI may be a significant contribution to the solution of this problem [138][139][140][141][142]. Success in this area may allow the creation of patterns for determining phenotypes and plant cultivars within one crop, which will become the basis for a database of hyperspectral portraits of plants.

If it could confidently detect different types of plant stresses and distinguish plants infected with pathogens from healthy one and/or those affected by abiotic stresses, it could study the influence of the genotypic characteristics of a pathogen on the spectral profile of an infected plant. To do this, it is necessary to identify the differences between plants of the same phenotype as affected by pathogens with different genotypes. Since, for many pathogens, primarily micromycetes, the intrageneric and even intraspecific diversity is extremely high, it is necessary to investigate the possible differences in the spectral manifestations of symptoms, for example, between different species of fungi of the genus *Fusarium* or between different races of the brown rust pathogen (*Puccinia triticina*). The aim of such experiment will be to study the effect of the phenotypic and genotypic diversity of pathogens on the variability of spectral portraits of host plants. The visual manifestations of symptoms of yellow rust (*Puccinia striiformis*) caused by different races or different strains of *Fusarium graminearum* are often very similar. In the early stages of the disease, chlorosis caused by pathogens of different species may have similar spectral portraits, which become more distinguishable in the later stages of the disease, and, thus, is also an important direction for research [57][60][143][67][55][56][63][69][73][77][78][79][80][81]. The influence of plant resistance on the symptomatology of pathogenesis and works describing the difference in the data obtained in such cases is also worth mentioning [63][69][73][74][78][79][81][85][86][92][93][89][88]. The determination of resistant cultivars using hyperspectral sensing is also a promising area of research with great applied potential [78].

One more direction, which is important for the early detection of plant diseases using HRS, is the study of spectral portraits of pathogens themselves. Unfortunately, this is only possible for a small number of diseases, such as wheat powdery mildew caused by *Blumeria graminis* and wheat yellow rust of wheat caused by *Puccinia striiformis*, which show characteristic external symptoms in the early stages. Usually, these are diseases of fungal origin, where the object of detection is *micromycete mycelium* or spores on the leaf surface of a diseased plant. Disease detection by this method is considered in the example of wheat yellow rust, using pure fungal spore spectra as reference [90].

Pest control is also an important aspect of plant protection. It was hypothesized that HRS can also be used to early detect such dangerous pests as the Colorado potato beetle (*Leptinotarsa decemlineata*), sunn pest (*Eurygaster integriceps*) [144],

or western corn rootworm (*Diabrotica virgifera virgifera*), using spectral portraits of imago and different ages of larvae. Currently, a small number of works have been published on this topic [126][144][145][146][147][148], but we consider this direction to be very promising, especially for use in industrial greenhouses. Another possible direction of research is the detection of local outbreaks of pests outside farmlands, for example, locusts (*Acridoidea*) or beet webworms (*Loxostege sticticalis*), in order to eliminate them early before these pests can cause damage to yields.

It was believed that the effect of biochemical changes in plant tissues is critical for the early detection of plant diseases using passive sensors. The reflectance of light from plants leaves is dependent on multiple biophysical and biochemical interactions. The VIS range (400–700 nm) is influenced by pigment content. The NIR range (700–1100 nm) is influenced by leaf structure, internal scattering processes and by the light absorption by leaf water. The SWIR range (1100–2500) is influenced by chemicals and water composition [132][149][150][151][152][153][154].

The most investigated areas in this topic are the determination of changes in the content of water, nitrogen (N) in plants, as well as of chlorophyll or carotenoids, using various SVIs, which can be used to detect plant diseases. These techniques can be used to determine the nitrogen content of plants [155][156][157] and to detect plant stresses and diseases [35][37][49][158][159][160], including the early detection of plant diseases and pest infestations [90][161][162][163][164].

The topic of detecting individual chemical elements or chemical compounds, including volatiles, in plants is a less studied problem. In plant physiology, such elements are of great importance, such as nitrogen (N), one of the key components for chlorophyll; phosphorus (in the monovalent orthophosphate form $H_2PO_4^-$), a key macronutrient; potassium (K^+), influencing leaf color; calcium (Ca^{2+}), which plays a fundamental physiological role in leaf structure and signaling; magnesium (Mg^{2+}), an essential macronutrient for photosynthesis (as it is the central atom of chlorophyll); sulfur (S), in the form of sulfate; iron (Fe^{2+} or Fe^{3+}), copper (Cu^{2+}), manganese (Mn^{2+}) and zinc (Zn^{2+}), which are essential elements for plant growth and components of many enzymes; and the ions responsible for salination: Na^+, K^+, Ca^{2+}, Mg^{2+} and Cl^- [154]. The detection of these elements by HRS can be a key factor for identifying plant diseases at an early stage, since plant diseases are accompanied by a deficiency of some of the listed elements, which is the cause of chlorotic and necrotic changes in plant tissues [154]. Unfortunately, this task is difficult and poorly studied, but the following works prove the possibility of determining the chemical composition of plants in the VIS, NIR and SWIR ranges. Pandey et al. detected a wide range of macronutrients, namely N, P, K, Mg, Ca and S, and micronutrients, namely Fe, Mn, Cu and Zn, in maize and soybean plants [165]. Zhou et al. detected cadmium (Cd) concentrations in brown rice before harvest [166]. Ge et al. tried to analyze chlorophyll content (CHL), leaf water content (LWC), specific leaf area (SLA), nitrogen (N), phosphorus (P) and potassium (K) in maize using different SVIs but succeeded only with CHL and N [167]. Hu et al. proved to determine the content of Ca, Mg, Mo and Zn in wheat kernels [168].

The most difficult and interesting direction is the detection of the content of not individual elements, but more complex chemical compounds using HRS. As an example of such works, one can cite the articles by Gold et al., where the mechanisms of physiological changes in potato plants were considered when inoculated by *Alternaria solani* and *Phytophthora infestans* pathogens in the analytical example of the contents of foliar nitrogen, total phenolics, sugar and starch [73][74]. Fuentes et al. monitored the chemical fingerprints of different leaf samples and studied the correlation of aphid numbers in wheat plants with the presence and quantity alcohol, methane, hydrogen peroxide, aromatic compounds and amide functional groups compounds [169]. The paper [169] presented results on the implementation of SWIR HRS (1596–2396 nm) and a low-cost electronic nose (e-nose) coupled with machine learning. The authors believe that such study of plant physiology models open their use to assessing models of other biotic and abiotic stress effects on plants. Thus, the search for plant diseases at early stages using passive sensors, including hyperspectral ones, should be carried out in three main directions: the search for the characteristic immune response of the host plant to the pathogen, the search for characteristic symptoms of plant damage by the pathogen or the search for spectral portraits of the pathogen or pest itself. It is always necessary to take into account other stress factors affecting the spectral portrait of a diseased plant, which will allow us to accurately determine plant diseases using passive remote sensing.

Further development of experiment planning should be considered, preferably using a common methodology, so that there is an opportunity to adequately compare the results. An experiment tree, which will consider the physiological parameters of the plant should be designed [170]. All phases of the experiment should be considered and planned in advance, on the basis of the science of experiment planning, which is sufficiently well developed for applied physical research, based on the methods of probability theory and mathematical statistics. The following research phases for each type of sensors should be developed: laboratory research in deterministic conditions of deterministic parameters; the allocation of spectral bands responsible for certain parameters of plants (including diseases) in laboratory experiments; repetition (possibly multiple) of a laboratory experiment to collect statistics and validate; transfer of the experiment to field conditions to verify the correctness of the selected spectral bands. Such planning of experiments and the creation of a

methodology for conducting them fills in the gaps associated with the lack of consideration of such factors as: different phenotypes of plants and their different spectral responses; various diseases and also their different spectral responses; the need to create and take into account a model of light propagation from an irradiating source to normalize hyperspectral imagery data [170][171][172][173].

References

1. Elad, Y.; Pertot, I. Climate change impacts on plant pathogens and plant diseases. J. Crop Improv. 2014, 28, 99–139.
2. Mahlein, A.K.; Kuska, M.T.; Behmann, J.; Polder, G.; Walter, A. Hyperspectral sensors and imaging technologies in phytopathology: State of the art. Annu. Rev. Phytopathol. 2018, 56, 535–558.
3. Weiss, M.; Jacob, F.; Duveiller, G. Remote sensing for agricultural applications: A meta-review. Remote Sens. Environ. 2020, 236, 111402.
4. Liu, J.; Miller, J.R.; Haboudane, D.; Pattey, E.; Nolin, M.C. Variability of seasonal CASI image data products and potential application for management zone delineation for precision agriculture. Can. J. Remote Sens. 2005, 31, 400–411.
5. Jensen, J.R. Remote Sensing of the Environment: An Earth Resource Perspective; Prentice Hall: Upper Saddle River, NJ, USA, 2006.
6. Jones, H.G.; Vaughan, R.A. Remote Sensing of Vegetation: Principles, Techniques, and Applications; Oxford University Press: Oxford, UK, 2010.
7. Lucieer, A.; Malenovský, Z.; Veness, T.; Wallace, L. HyperUAS-imaging spectroscopy from a multirotor unmanned aircraft system. J. Field Robot. 2014, 31, 571–590.
8. Gonzalez-Dugo, V.; Hernandez, P.; Solis, I.; Zarco-Tejada, P. Using High-Resolution Hyperspectral and Thermal Airborne Imagery to Assess Physiological Condition in the Context of Wheat Phenotyping. Remote Sens. 2015, 7, 13586–13605.
9. Adao, T.; Hruška, J.; Pádua, L.; Bessa, J.; Peres, E.; Morais, R.; Sousa, J. Hyperspectral Imaging: A Review on UAV-Based Sensors, Data Processing and Applications for Agriculture and Forestry. Remote Sens. 2017, 9, 1110.
10. Metternicht, G. Vegetation indices derived from high-resolution airborne videography for precision crop management. Int. J. Remote Sens. 2003, 24, 2855–2877.
11. Schell, J.; Deering, D. Monitoring vegetation systems in the Great Plains with ERTS. NASA Spec. Publ. 1973, 351, 309.
12. Thomas, S.; Kuska, M.T.; Bohnenkamp, D.; Brugger, A.; Alisaac, E.; Wahabzada, M.; Behmann, J.; Mahlein, A.K. Benefits of hyperspectral imaging for plant disease detection and plant protection: A technical perspective. JPDP 2018, 125, 5–20.
13. De Jong, S.M.; Van Der Meer, F.D.; Clevers, J.G. Basics of Remote Sensing. Remote Sensing Image Analysis: Including the Spatial Domain; Springer: Dordrecht, The Netherlands, 2004.
14. Mishra, P.; Asaari, M.S.M.; Herrero-Langreo, A.; Lohumi, S.; Diezma, B.; Scheunders, P. Close range hyperspectral imaging of plants: A review. Biosyst. Eng. 2017, 164, 49–67.
15. Chen, Y.; Lin, Z.; Zhao, X.; Wang, G.; Gu, Y. Deep learning-based classification of hyperspectral data. IEEE J. Sel. Top. Appl. 2014, 7, 2094–2107.
16. Landgrebe, D.A. Signal Theory Methods in Multispectral Remote Sensing; John Wiley & Sons: Hoboken, NJ, USA, 2003.
17. Green, R.O.; Eastwood, M.L.; Sarture, C.M.; Chrien, T.G.; Aronsson, M.; Chippendale, B.J.; Faust, J.A.; Pavri, B.E.; Chovit, C.J.; Solis, M.; et al. Imaging spectroscopy and the airborne visible/infrared imaging spectrometer (AVIRIS). Remote Sens. Environ. 1998, 65, 227–248.
18. Chang, C.-I. Hyperspectral Imaging: Techniques for Spectral Detection and Classification; Kluwer/Plenum: New York, NY, USA, 2003.
19. Jia, X.; Richards, J.A.; Ricken, D.E. Remote Sensing Digital Image Analysis: An Introduction; Springer: Berlin/Heidelberg, Germany, 1999.
20. Serpico, S.B.; D'Inca, M.; Melgani, F.; Moser, G. Comparison of feature reduction techniques for classification of hyperspectral remote-sensing data. In Image and Signal Processing for Remote Sensing VIII; International Society for Optics and Photonics: Bellingham, WA, USA, 2003; Volume 4885, pp. 347–358.

21. Kaewpijit, S.; Le Moigne, J.; El-Ghazawi, T. Automatic reduction of hyperspectral imagery using wavelet spectral analysis. IEEE Trans. Geosci. Remote Sens. 2003, 41, 863–871.
22. Xie, C.; He, Y. Spectrum and image texture features analysis for early blight disease detection on eggplant leaves. Sensors 2016, 16, 676.
23. Barreto, A.; Paulus, S.; Varrelmann, M.; Mahlein, A.K. Hyperspectral imaging of symptoms induced by Rhizoctonia solani in sugar beet: Comparison of input data and different machine learning algorithms. J. Plant Dis. Prot. 2020, 127, 441–451.
24. Huang, L.; Zhang, H.; Ruan, C.; Huang, W.; Hu, T.; Zhao, J. Detection of scab in wheat ears using in situ hyperspectral data and support vector machine optimized by genetic algorithm. Int. J. Agric. Biol. Eng. 2020, 13, 182–188.
25. Nguyen, C.; Sagan, V.; Maimaitiyiming, M.; Maimaitijiang, M.; Bhadra, S.; Kwasniewski, M.T. Early Detection of Plant Viral Disease Using Hyperspectral Imaging and Deep Learning. Sensors 2021, 21, 742.
26. Liu, F.; Xiao, Z. Disease Spots Identification of Potato Leaves in Hyperspectral Based on Locally Adaptive 1D-CNN. In Proceedings of the 2020 IEEE International Conference on Artificial Intelligence and Computer Applications (ICAICA), Dalian, China, 27–29 June 2020.
27. Jin, X.; Jie, L.; Wang, S.; Qi, H.J.; Li, S.W. Classifying wheat hyperspectral pixels of healthy heads and Fusarium head blight disease using a deep neural network in the wild field. Remote Sens. 2018, 10, 395.
28. Hruška, J.; Adão, T.; Pádua, L.; Marques, P.; Peres, E.; Sousa, A.; Morais, R.; Sousa, J.J. Deep Learning-Based Methodological Approach for Vineyard Early Disease Detection Using Hyperspectral Data. In Proceedings of the IGARSS 2018-2018 IEEE International Geoscience and Remote Sensing Symposium, Valencia, Spain, 22–27 July 2018.
29. Shafri, H.Z.M.; Anuar, M.I. Hyperspectral Signal Analysis for Detecting Disease Infection in Oil Palms. In Proceedings of the International Conference on Computer and Electrical Engineering, Phuket, Thailand, 20–22 December 2008.
30. Shafri, H.Z.M.; Hamdan, N. Hyperspectral Imagery for Mapping Disease Infection in Oil Palm Plantation Using Vegetation Indices and Red Edge Techniques. Am. J. Appl. Sci. 2009, 6, 1031–1035.
31. Lelong, C.C.D.; Roger, J.-M.; Bregand, S.; Dubertret, F.; Lanore, M.; Sitorus, N.A.; Raharjo, D.A.; Caliman, J.-P. Discrimination of fungal disease infestation in oil-palm canopy hyperspectral reflectance data. In Proceedings of the First Workshop on Hyperspectral Image and Signal Processing: Evolution in Remote Sensing, Grenoble, France, 26–28 August 2009.
32. Lelong, C.C.D.; Roger, J.-M.; Bregand, S.; Dubertret, F.; Lanore, M.; Sitorus, N.; Raharjo, D.A.; Caliman, J.-P. Evaluation of Oil-Palm Fungal Disease Infestation with Canopy Hyperspectral Reflectance Data. Sensors 2010, 10, 734–747.
33. Shafri, H.Z.M.; Anuar, M.I.; Seman, I.A.; Noor, N.M. Spectral discrimination of healthy and Ganoderma-infected oil palms from hyperspectral data. Int. J. Remote Sens. 2011, 32, 7111–7129.
34. Liaghat, S.; Ehsani, R.; Mansor, S.; Shafri, H.Z.M.; Meon, S.; Sankaran, S.; Azam, S.H.M.N. Early detection of basal stem rot disease (Ganoderma) in oil palms based on hyperspectral reflectance data using pattern recognition algorithms. Int. J. Remote Sens. 2014, 35, 3427–3439.
35. Anuar, M.I.; Abu, S.I.; Nisfariza, M.N.; Nordiana, A.A.; Shafri, H.Z.M.; Ezzati, B. The development of spectral indices for early detection of Ganoderma disease in oil palm seedlings. Int. J. Remote Sens. 2017, 38, 6505–6527.
36. Ahmadi, P.; Muharam, F.M.; Ahmad, K.; Mansor, S.; Abu, S.I. Early Detection of Ganoderma Basal Stem Rot of Oil Palms Using Artificial Neural Network Spectral Analysis. Plant Dis. 2017, 101, 1009–1016.
37. Anuar, M.I.; Nisfariza, M.N.; Ezzati, B.; Idris, A.S.; Steven, M.D.; Boyd, D. Analysis of airborne hyperspectral image using vegetation indices, red edge position and continuum removal for detection of Ganoderma disease in oil palm. J. Oil Palm Res. 2018, 30, 416–428.
38. Azmi, A.N.N.; Bejo, S.K.; Jahari, M.; Muharam, F.M.; Yule, I.; Husin, N.A. Early Detection of Ganoderma boninense in Oil Palm Seedlings Using Support Vector Machines. Remote Sens. 2020, 12, 3920.
39. Selvaraja, S.; Balasundram, S.K.; Vadamalai, G.; Husni, M.H.A. Use of Spectral Reflectance to Discriminate between Potassium Deficiency and Orange Spotting Symptoms in Oil Palm (Elaeis guineensis). Life Sci. J. 2013, 10, 947–951.
40. Selvaraja, S.; Balasundram, S.K.; Vadamalai, G.; Husni, M.H.A.; Khosla, R. Remote Sensing as a Tool to Assess Orange Spotting Disease in Oil Palm (Elaies guineensis). Mitt. Klosterneubg. 2014, 64, 12–26.
41. Golhani, K.; Balasundram, S.K.; Vadamalai, G.; Pradhan, B. A review of neural networks in plant disease detection using hyperspectral data. Inf. Process. Agric. 2018, 5, 354–371.

42. Golhani, K.; Balasundram, S.K.; Vadamalai, G.; Pradhan, B. Use of reflectance spectroscopy as a tool for screening viroid-inoculated oil palm seedlings. OAJAR 2017, 2, 1–4.

43. Golhani, K.; Balasundram, S.K.; Vadamalai, G.; Pradhan, B. Selection of a spectral index for detection of orange spotting disease in oil palm (Elaeis guineensis jacq.) using red edge and neural network techniques. J. Indian Soc. Remote Sens. 2019, 47, 639–646.

44. Sankaran, S.; Mishra, A.; Maja, J.M.; Ehsani, R. Visible-near infrared spectroscopy for detection of Huanglongbing HLB) Using a VIS-NIR Spectroscopy Technique. Comput. Electron. Agric. 2011, 77, 127–134.

45. Sankaran, S.; Ehsani, R. Visible-near infrared spectroscopy based citrus greening detection: Evaluation of spectral feature extraction techniques. Crop Prot. 2011, 30, 1508–1513.

46. Sankaran, S.; Maja, J.; Buchanon, S.; Ehsani, R. Huanglongbing (Citrus Greening) Detection Using Visible, Near Infrared and Thermal Imaging Techniques. Sensors 2013, 13, 2117–2130.

47. Li, X.; Lee, W.S.; Li, M.; Ehsani, R.; Mishra, A.R.; Yang, C.; Mangan, R.L. Spectral difference analysis and airborne imaging classification for citrus greening infected trees. Comput. Electron. Agric. 2012, 83, 32–46.

48. Kumar, A.; Lee, W.S.; Ehsani, R.J.; Albrigo, L.G.; Yang, C.; Mangane, R.L. Citrus greening disease detection using aerial hyperspectral and multispectral imaging techniques. J. Appl. Remote Sens. 2012, 6, 063542.

49. Weng, H.; Lu, J.; Cen, H.; He, M.; Zeng, Y.; Hua, S.; Li, H.; Meng, Y.; Fang, H.; He, Y. Hyperspectral reflectance imaging combined with carbohydrate metabolism analysis for diagnosis of citrus Huanglongbing in different seasons and cultivars. Sens. Actuators B Chem. 2018, 275, 50–60.

50. Deng, X.; Zhu, Z.; Yang, J.; Zheng, Z.; Huang, Z.; Yin, X.; Wei, S.; Lan, Y. Detection of Citrus Huanglongbing Based on Multi-Input Neural Network Model of UAV HRS. Remote Sens. 2020, 12, 2678.

51. Deng, X.; Huang, Z.; Zheng, Z.; Lan, Y.; Dai, F. Field detection and classification of citrus Huanglongbing based on hyperspectral reflectance. Comput. Electron. Agric. 2019, 167, 105006.

52. Mei, H.; Deng, X.; Hong, T.; Luo, X.; Deng, X. Early detection and grading of citrus huanglongbing using hyperspectral imaging technique. Trans. Chin. Soc. Agric. Eng. 2014, 30, 140–147.

53. Zhang, M.; Qin, Z.; Liu, X.; Ustin, S.L. Detection of stress in tomatoes induced by late blight disease in California, USA, using HRS. Int. J. Appl. Earth. Obs. 2003, 4, 295–310.

54. Krezhova, D.; Dikova, B.; Maneva, S. Ground based HRS for disease detection of tobacco plants. Bulg. J. Agric. Sci. 2014, 20, 1142–1150.

55. Xie, C.; Shao, Y.; Li, X.; He, Y. Detection of early blight and late blight diseases on tomato leaves using hyperspectral imaging. Sci. Rep. 2015, 5, 16564.

56. Xie, C.; Yang, C.; He, Y. Hyperspectral imaging for classification of healthy and gray mold diseased tomato leaves with different infection severities. Comput. Electron. Agric. 2017, 135, 154–162.

57. Lu, J.; Zhou, M.; Gao, Y.; Jiang, H. Using hyperspectral imaging to discriminate yellow leaf curl disease in tomato leaves. Precis. Agric. 2017, 19, 379–394.

58. Zhu, H.; Cen, H.; Zhang, C.; He, Y. Early Detection and Classification of Tobacco Leaves Inoculated with Tobacco Mosaic Virus Based on Hyperspectral Imaging Technique. In Proceedings of the ASABE Annual International Meeting, Orlando, FL, USA, 17–20 July 2016.

59. Zhu, H.; Chu, B.; Zhang, C.; Liu, F.; Jiang, L.; He, Y. Hyperspectral imaging for presymptomatic detection of tobacco disease with successive projections algorithm and machine-learning classifiers. Sci. Rep. 2017, 7, 4125.

60. Lu, J.; Ehsani, R.; Shi, Y.; de Castro, A.I.; Wang, S. Detection of multi-tomato leaf diseases (late blight, target and bacterial spots) in different stages by using a spectral-based sensor. Sci. Rep. 2018, 8, 2793.

61. Wang, D.; Vinson, R.; Holmes, M.; Seibel, G.; Bechar, A.; Nof, S.; Luo, Y.; Tao, Y. Early Tomato Spotted Wilt Virus Detection using Hyperspectral Imaging Technique and Outlier Removal Auxiliary Classifier Generative Adversarial Nets (OR-AC-GAN). In Proceedings of the ASABE Annual International Meeting, Detroit, MI, USA, 29 July–1 August 2018.

62. Griffel, L.M.; Delparte, D.; Edwards, J. Using Support Vector Machines classification to differentiate spectral signatures of potato plants infected with Potato Virus Y. Comput. Electron. Agric. 2018, 153, 318–324.

63. Bienkowski, D.; Aitkenhead, M.J.; Lees, A.K.; Gallagher, C.; Neilson, R. Detection and differentiation between potato (Solanum tuberosum) diseases using calibration models trained with non-imaging spectrometry data. Comput. Electron. Agric. 2019, 167, 105056.

64. Gu, Q.; Sheng, L.; Zhang, T.; Lu, Y.; Zhang, Z.; Zheng, K.; Hu, H.; Zhou, H. Early detection of tomato spotted wilt virus infection in tobacco using the hyperspectral imaging technique and machine learning algorithms. Comput. Electron. Agric. 2019, 167, 105066.

65. Polder, G.; Blok, P.M.; de Villiers, H.A.C.; Van der Wolf, J.M.; Kamp, J. Potato Virus Y Detection in Seed Potatoes Using Deep Learning on Hyperspectral Images. Front. Plant Sci. 2019, 10, 209.

66. Van de Vijvera, R.; Mertensa, K.; Heungensb, K.; Somersc, B.; Nuyttensa, D.; Borra-Serranoc, I.; Lootensd, P.; Roldán-Ruizd, I.; Vangeytea, J.; Saeys, W. In-field detection of Alternaria solani in potato crops using hyperspectral imaging. Comput. Electron. Agric. 2019, 168, 105106.

67. Abdulridha, J.; Ampatzidis, Y.; Kakarla, S.C.; Robert, P. Laboratory and UAV-Based Identification and Classification of Tomato Yellow Leaf Curl, Bacterial Spot, and Target Spot Diseases in Tomato Utilizing Hyperspectral Imaging and Machine Learning. Remote Sens. 2020, 21, 3843.

68. Wang, D.; Vinson, R.; Holmes, M.; Seibel, G.; Bechar, A.; Nof, S.; Tao, Y. Early Detection of Tomato Spotted Wilt Virus by Hyperspectral Imaging and Outlier Removal Auxiliary Classifier Generative Adversarial Nets (OR-AC-GAN). Sci. Rep. 2019, 9, 4377.

69. Franceschini, M.H.D.; Bartholomeus, H.; van Apeldoorn, D.F.; Suomalainen, J.; Kooistra, L. Feasibility of unmanned aerial vehicle optical imagery for early detection and severity assessment of late blight in potato. Remote Sens. 2019, 11, 224.

70. Morellos, A.; Tziotzios, G.; Orfanidou, C.; Pantazi, X.E.; Sarantaris, C.; Maliogka, V.; Alexandridis, T.K.; Moshou, D. Non-Destructive Early Detection and Quantitative Severity Stage Classification of Tomato Chlorosis Virus (ToCV) Infection in Young Tomato Plants Using Vis–NIR Spectroscopy. Remote Sens. 2020, 12, 1920.

71. Fernandez, C.I.; Leblon, B.; Haddadi, A.; Wang, J.; Wang, K. Potato Late Blight Detection at the Leaf and Canopy Level Using Hyperspectral Data. Can. J. Remote Sens. 2020, 46, 390–413.

72. Fernandez, C.I.; Leblon, B.; Haddadi, A.; Wang, K.; Wang, J. Potato Late Blight Detection at the Leaf and Canopy Levels Based in the Red and Red-Edge Spectral Regions. Remote Sens. 2020, 12, 1292.

73. Gold, K.M.; Townsend, P.A.; Herrmann, I.; Gevens, A.J. Investigating potato late blight physiological differences across potato cultivars with spectroscopy and machine learning. Plant Sci. 2019, 110316.

74. Gold, K.M.; Townsend, P.A.; Chlus, A.; Herrmann, I.; Couture, J.J.; Larson, E.R.; Gevens, A.J. Hyperspectral Measurements Enable Pre-Symptomatic Detection and Differentiation of Contrasting Physiological Effects of Late Blight and Early Blight in Potato. Remote Sens. 2020, 12, 286.

75. Delwiche, S.R.; Kim, M.S. Biological Quality and Precision Agriculture, II. DeShazer, J.A., Meyer, G.E., Eds.; SPIE: Bellingham, WA, USA, 2000; Volume 4203.

76. Bauriegel, E.; Giebel, A.; Geyer, M.; Schmidt, U.; Herppich, W.B. Early detection of Fusarium infection in wheat using hyper-spectral imaging. Comput. Electron. Agric. 2011, 75, 304–312.

77. Barbedo, J.G.A.; Tibola, C.S.; Fernandes, J.M.C. Detecting Fusarium head blight in wheat kernels using hyperspectral imaging. Biosyst. Eng. 2015, 131, 65–76.

78. Alisaac, E.; Behmann, J.; Kuska, M.T.; Dehne, H.-W.; Mahlein, A.-K. Hyperspectral quantification of wheat resistance to Fusarium head blight: Comparison of two Fusarium species. Eur. J. Plant Pathol. 2018, 152, 869–884.

79. Mahlein, A.-K.; Alisaac, E.; Al Masri, A.; Behmann, J.; Dehne, H.-W.; Oerke, E.-C. Comparison and Combination of Thermal, Fluorescence, and Hyperspectral Imaging for Monitoring Fusarium Head Blight of Wheat on Spikelet Scale. Sensors 2019, 19, 2281.

80. Whetton, R.L.; Hassall, K.L.; Waine, T.W.; Mouazen, A.M. Hyperspectral measurements of yellow rust and fusarium head blight in cereal crops: Part 1: Laboratory study. Biosyst. Eng. 2018, 166, 101–115.

81. Whetton, R.L.; Waine, T.W.; Mouazen, A.M. Hyperspectral measurements of yellow rust and fusarium head blight in cereal crops: Part 2: On-line field measurement. Biosyst. Eng. 2018, 167, 144–158.

82. Ma, H.; Huang, W.; Jing, Y.; Pignatti, S.; Laneve, G.; Dong, Y.; Ye, H.; Liu, L.; Guo, A.; Jiang, J. Identification of Fusarium Head Blight in Winter Wheat Ears Using Continuous Wavelet Analysis. Sensors 2019, 20, 20.

83. Zhang, N.; Pan, Y.; Feng, H.; Zhao, X.; Yang, X.; Ding, C.; Yang, G. Development of Fusarium head blight classification index using hyperspectral microscopy images of winter wheat spikelets. Biosyst. Eng. 2019, 186, 83–99.

84. Zhang, D.; Wang, Q.; Lin, F.; Yin, X.; Gu, C.; Qiao, H. Development and Evaluation of a New Spectral Disease Index to Detect Wheat Fusarium Head Blight Using Hyperspectral Imaging. Sensors 2020, 20, 2260.

85. Huang, W.; Lamb, D.W.; Niu, Z.; Zhang, Y.; Liu, L.; Wang, J. Identification of yellow rust in wheat using in-situ spectral reflectance measurements and airborne hyperspectral imaging. Precis. Agric. 2007, 8, 187–197.

86. Zhang, J.; Pu, R.; Huang, W.; Yuan, L.; Luo, J.; Wang, J. Using in-situ hyperspectral data for detecting and discriminating yellow rust disease from nutrient stresses. Field Crops Res. 2012, 134, 165–174.

87. Krishna, G.; Sahoo, R.N.; Pargal, S.; Gupta, V.K.; Sinha, P.; Bhagat, S.; Saharan, M.S.; Singh, R.; Chattopadhyay, C. Assessing Wheat Yellow Rust Disease through Hyperspectral Remote Sensing. ISPRS Int. Arch. Photogramm. Remote Sens. Spat. Inf. Sci. 2014, XL-8, 1413–1416.
88. Zheng, Q.; Huang, W.; Cui, X.; Dong, Y.; Shi, Y.; Ma, H.; Liu, L. Identification of Wheat Yellow Rust Using Optimal Three-Band Spectral Indices in Different Growth Stages. Sensors 2018, 19, 35.
89. Bohnenkamp, D.; Behmann, J.; Mahlein, A.-K. In-Field Detection of Yellow Rust in Wheat on the Ground Canopy and UAV Scale. Remote Sens. 2019, 11, 2495.
90. Bohnenkamp, D.; Kuska, M.T.; Mahlein, A.-K.; Behmann, J. Utilising pure fungal spore spectra as reference for a hyperspectral signal decomposition and symptom detection of wheat rust diseases on leaf scale. Plant Pathol. 2019, 68, 1188–1195.
91. Zhang, X.; Han, L.; Dong, Y.; Shi, Y.; Huang, W.; Han, L.; González-Moreno, P.; Ma, H.; Ye, H.; Sobeih, T. A Deep Learning-Based Approach for Automated Yellow Rust Disease Detection from High-Resolution Hyperspectral UAV Images. Remote Sens. 2019, 11, 1554.
92. Guo, A.; Huang, W.; Ye, H.; Dong, Y.; Ma, H.; Ren, Y.; Ruan, C. Identification of Wheat Yellow Rust Using Spectral and Texture Features of Hyperspectral Images. Remote Sens. 2020, 12, 1419.
93. Guo, A.; Huang, W.; Dong, Y.; Ye, H.; Ma, H.; Liu, B.; Wu, B.; Ren, Y.; Ruan, C.; Geng, Y. Wheat Yellow Rust Detection Using UAV-Based Hyperspectral Technology. Remote Sens. 2021, 13, 123.
94. Lan, Y.; Zhu, Z.; Deng, X.; Lian, B.; Huang, J.; Huang, Z.; Hu, J. Monitoring and classification of Huanglongbing plants of citrus based on UAV HRS. Trans. Chin. Soc. Agric. Eng. 2019, 35, 92–100.
95. Lan, Y.; Huang, Z.; Deng, X.; Zhu, Z.; Huang, H.; Zheng, Z.; Lian, B.; Zeng, G.; Tong, Z. Comparison of machine learning methods for citrus greening detection on UAV multispectral images. Comput. Electron. Agric. 2020, 171, 105234.
96. Anuar, M.I. Modified vegetation indices for Ganoderma disease detection in oil palm from field spectroradiometer data. J. Appl. Remote Sens. 2009, 3, 033556.
97. Mansour, K.; Mutanga, O.; Adam, E.; Abdel-Rahman, E.M. Multispectral remote sensing for mapping grassland degradation using the key indicators ofgrass species and edaphic factors. Geocarto Int. 2016, 31, 477–491.
98. Martínez-Usó, A.; Pla, F.; Sotoca, J.M.; García-Sevilla, P. Clustering-based hyperspectral band selection using information measures. IEEE Trans. Geosci. Remote 2007, 45, 4158–4171.
99. Guo, B.F.; Damper, R.I.; Gunn, S.R.; Nelson, J.D.B. A fast separability-based feature-selection method for high-dimensional remotely sensed image classification. Pattern Recogn. 2008, 41, 1653–1662.
100. Lorente, D.; Aleixos, N.; Gómez-Sanchis, J.; Cubero, S.; Blasco, J. Selection of optimal wavelengths features for decay detection in citrus fruit using the ROC curve and neural networks. Food Bioprocess Technol. 2013, 6, 530–541.
101. Andries, J.P.M.; Heyden, Y.V.; Buydens, L.M.C. Predictive-property-ranked variable reduction in partial least squares modelling with final complexity adapted models: Comparison of properties for ranking. Anal. Chim. Acta 2013, 760, 34–45.
102. Van der Plank, J.E. Plant Diseases: Epidemics and Control; Academic: New York, NY, USA, 1963.
103. Wheeler, B.E.J. An Introduction to Plant Diseases; John Wiley: London, UK, 1969.
104. Hale, M.G.; Orcutt, D.M. The Physiology of Plants Under Stress; John Wiley & Sons: New York, NY, USA, 1987.
105. Fox, R.; Narra, H. Plant disease diagnosis. In The Epidemiology of Plant Diseases, 2nd ed.; Cooke, B.M., Jones, D.G., Kaye, B., Eds.; Springer: Dordrecht, The Netherlands, 2006; pp. 1–42.
106. Afanasenko, O.S.; Mironenko, N.V.; Bespalova, L.A.; Ablova, I.B.; Lashina, N.M. Ramularia spot blotch in Russian Federation: Distribution and diagnosis. Mikol. Fitopatol. 2019, 53, 236–245.
107. Kolander, T.M.; Bienapfl, J.C.; Kurle, J.E.; Malvick, D.K. Symptomatic and Asymptomatic Host Range of Fusarium virguliforme, the Causal Agent of Soybean Sudden Death Syndrome. Plant Dis. 2012, 96, 1148–1153.
108. Bray, E.A. Plant responses to water deficit. Trends Plant Sci. 1997, 2, 48–54.
109. Bohnert, H.J.; Sheveleva, E. Plant stress adaptations—Making metabolism move. Curr. Opin. Plant Biol. 1998, 1, 267–274.
110. Shabala, S. Plant Stress Physiology. CAB International: Oxford, UK; Oxford, MS, USA, 2012.
111. Senaratna, T.; Touchell, D.; Bunn, E.; Dixon, K. Acetyl salicylic acid (Aspirin) and salicylic acid induce multiple stress tolerance in bean and tomato plants. Plant Growth Regul. 2000, 30, 157–161.

112. Khan, M.I.R.; Fatma, M.; Per, T.S.; Anjum, N.A.; Khan, N.A. Salicylic acid-induced abiotic stress tolerance and underlying mechanisms in plants. Front. Plant Sci. 2015, 6, 462.

113. Koo, Y.M.; Heo, A.Y.; Choi, H.W. Salicylic Acid as a Safe Plant Protector and Growth Regulator. Plant Pathol. J. 2020, 36, 1–10.

114. Wasternack, C.; Hause, B. Jasmonates and octadecanoids: Signals in plant stress responses and development. Prog. Nucleic Acid Res. Mol. Biol. 2002, 165–221.

115. Dar, T.A.; Uddin, M.; Khan, M.M.A.; Hakeem, K.R.; Jaleel, H. Jasmonates counter plant stress: A Review. Environ. Exp. Bot. 2015, 115, 49–57.

116. Goel, P.; Prasher, S.; Landry, J.; Patel, R.; Bonnell, R.; Viau, A.; Miller, J. Potential of airborne hyperspectral remote sensing to detect nitrogen deficiency and weed infestation in corn. Comput. Electron. Agric. 2003, 38, 99–124.

117. Behmann, J.; Steinrücken, J.; Plümer, L. Detection of early plant stress responses in hyperspectral images. ISPRS J. Photogramm. Remote Sens. 2014, 93, 98–111.

118. Zhao, F.; Huang, Y.; Guo, Y.; Reddy, K.; Lee, M.; Fletcher, R.; Thomson, S. Early Detection of Crop Injury from Glyphosate on Soybean and Cotton Using Plant Leaf Hyperspectral Data. Remote Sens. 2014, 6, 1538–1563.

119. Huang, Y.; Yuan, L.; Reddy, K.N.; Zhang, J. In-situ plant hyperspectral sensing for early detection of soybean injury from dicamba. Biosyst. Eng. 2016, 149, 51–59.

120. Sayyari, M.; Salehi, F.; Valero, D. New Approaches to Modeling Methyl Jasmonate Effects on Pomegranate Quality during Postharvest Storage. Int. J. Fruit Sci. 2017, 17, 374–390.

121. Do Prado Ribeiro, L.; Klock, A.L.S.; Filho, J.A.W.; Tramontin, M.A.; Trapp, M.A.; Mithöfer, A.; Nansen, C. Hyperspectral imaging to characterize plant–plant communication in response to insect herbivory. Plant Methods 2018, 14, 54.

122. Zovko, M.; Žibrat, U.; Knapič, M.; Kovačić, M.B.; Romić, D. Hyperspectral remote sensing of grapevine drought stress. Precis. Agric. 2019, 20, 335–347.

123. Wang, J.; Zhang, C.; Shi, Y.; Long, M.; Islam, F.; Yang, C.; He, Y.; Zhou, W. Evaluation of quinclorac toxicity and alleviation by salicylic acid in rice seedlings using ground-based visible/near-infrared hyperspectral imaging. Plant Methods 2020, 16, 30.

124. Jackson, R.D. Remote Sensing of Biotic and Abiotic Plant Stress. Annu. Rev. Phytopathol. 1986, 24, 265–287.

125. Irmak, S.; Haman, D.Z.; Bastug, R. Determination of Crop Water Stress Index for Irrigation Timing and Yield Estimation of Corn. J. Agron. 2000, 92, 1221.

126. Nansen, C.; Macedo, T.; Swanson, R.; Weaver, D.K. Use of spatial structure analysis of hyperspectral data cubes for detection of insect-induced stress in wheat plants. Int. J. Remote Sens. 2009, 30, 2447–2464.

127. Lowe, A.; Harrison, N.; French, A.P. Hyperspectral image analysis techniques for the detection and classification of the early onset of plant disease and stress. Plant Methods 2017, 13, 80.

128. Nansen, C.; Sidumo, A.J.; Capareda, S. Variogram Analysis of Hyperspectral Data to Characterize the Impact of Biotic and Abiotic Stress of Maize Plants and to Estimate Biofuel Potential. Appl. Spectrosc. 2010, 64, 627–636.

129. Susič, N.; Žibrat, U.; Širca, S.; Strajnar, P.; Razinger, J.; Knapič, M.; Voncuna, A.; Urek, G.; Gerič Stare, B. Discrimination between abiotic and biotic drought stress in tomatoes using hyperspectral imaging. Sens. Actuators B Chem. 2018, 273, 842–852.

130. Das, B.; Mahajan, G.R.; Singh, R. HRS: Use in Detecting Abiotic Stresses in Agriculture. Adv. Crop. Environ. Interact. 2018, 317–335.

131. Gagkaeva, T.; Gavrilova, O.; Orina, A.; Lebedin, Y.; Shanin, I.; Petukhov, P.; Eremin, S. Analysis of Toxigenic Fusarium Species Associated with Wheat Grain from Three Regions of Russia: Volga, Ural, and West Siberia. Toxins 2019, 11, 252.

132. Mahlein, A.-K. Plant Disease Detection by Imaging Sensors—Parallels and Specific Demands for Precision Agriculture and Plant Phenotyping. Plant Dis. 2016, 100, 241–251.

133. Behmann, J.; Acebron, K.; Emin, D.; Bennertz, S.; Matsubara, S.; Thomas, S.; Bohnenkamp, D.; Kuska, M.T.; Jussila, J.; Salo, H.; et al. Specim IQ: Evaluation of a new, miniaturized handheld hyperspectral camera and its application for plant phenotyping and disease detection. Sensors 2018, 18, 441.

134. Singh, A.K.; Ganapathysubramanian, B.; Sarkar, S.; Singh, A. Deep Learning for Plant Stress Phenotyping: Trends and Future Perspectives. Trends Plant Sci. 2018, 23, 883–898.

135. Brugger, A.; Behmann, J.; Paulus, S.; Luigs, H.-G.; Kuska, M.T.; Schramowski, P.; Kersting, K.; Steiner, U.; Mahlein, A.-K. Extending Hyperspectral Imaging for Plant Phenotyping to the UV-Range. Remote Sens. 2019, 11, 1401.

136. Mutka, A.M.; Bart, R.S. Image-based phenotyping of plant disease symptoms. Front. Plant Sci. 2015, 5, 734.

137. Mutka, A.M.; Fentress, S.J.; Sher, J.W.; Berry, J.C.; Pretz, C.; Nusinow, D.A.; Bart, R. Quantitative, Image-Based Phenotyping Methods Provide Insight into Spatial and Temporal Dimensions of Plant Disease. Plant Physiol. 2016, 172, 650–660.

138. Calderón, R.; Navas-Cortés, J.A.; Lucena, C.; Zarco-Tejada, P.J. High-resolution airborne hyperspectral and thermal imagery for early detection of Verticillium wilt of olive using fluorescence, temperature and narrow-band spectral indices. Remote Sens. Environ. 2013, 139, 231–245.

139. Roháček, K.; Soukupová, J.; Barták, M. Chlorophyll fluorescence: A wonderful tool to study plant physiology and plant stress. Res. Signpost. 2008, 37, 41–104.

140. Bauriegel, E.; Giebel, A.; Herppich, W.B. Hyperspectral and Chlorophyll Fluorescence Imaging to Analyse the Impact of Fusarium culmorum on the Photosynthetic Integrity of Infected Wheat Ears. Sensors 2011, 11, 3765–3779.

141. Yu, K.; Leufen, G.; Hunsche, M.; Noga, G.; Chen, X.; Bareth, G. Investigation of Leaf Diseases and Estimation of Chlorophyll Concentration in Seven Barley Varieties Using Fluorescence and Hyperspectral Indices. Remote Sens. 2013, 6, 64–86.

142. Pérez-Bueno, M.L.; Pineda, M.; Barón, M. Phenotyping Plant Responses to Biotic Stress by Chlorophyll Fluorescence Imaging. Front. Plant Sci. 2019, 10, 1135.

143. Abdulridha, J.; Ampatzidis, Y.; Qureshi, J.; Robert, P. Detection of target spot and bacterial spot diseases in tomato using UAV based and benchtop based hyperspectral imaging techniques. Precis. Agric. 2019, 21, 955–978.

144. Basati, Z.; Jamshidi, B.; Rasekh, M.; Abbaspour-Gilandeh, Y. Detection of sunn pest-damaged wheat samples using visible/near-infrared spectroscopy based on pattern recognition. Spectrochim. Acta A Mol. Biomol. Spectrosc. 2018, 203, 308–314.

145. Kumar, J.; Vashisth, A.; Sehgal, V.K.; Gupta, V.K. Assessment of Aphid Infestation in Mustard by Hyperspectral Remote Sensing. J. Indian Soc. Remote Sens. 2012, 41, 83–90.

146. Canário, D.V.P.; Figueiredo, E.; Franco, J.C.; Guerra, R. Detecting early mealybug infestation stages on tomato plants using optical spectroscopy. Eur. J. Hortic. Sci. 2017, 82, 141–148.

147. Zhang, J.; Huang, Y.; Pu, R.; Gonzalez-Moreno, P.; Yuan, L.; Wu, K.; Huang, W. Monitoring plant diseases and pests through remote sensing technology: A review. Comput. Electron. Agric. 2019, 165, 104943.

148. Yan, T.; Xu, W.; Lin, J.; Duan, L.; Gao, P.; Zhang, C.; Lu, X. Combining Multi-Dimensional Convolutional Neural Network (CNN) With Visualization Method for Detection of Aphis gossypii Glover Infection in Cotton Leaves Using Hyperspectral Imaging. Front. Plant Sci. 2021, 12, 74.

149. Carter, G.A.; Knapp, A.K. Leaf optical properties in higher plants: Linking spectral characteristics to stress and chlorophyll concentration. Am. J. Bot. 2001, 88, 677–684.

150. Gitelson, A.A.; Merzlyak, N.M.; Chivkunova, B.O. Optical properties and non-destructive estimation of anthocyanin content in plant leaves. Photochem. Photobiol. 2001, 74, 38–45.

151. Carter, G.A.; Spiering, B.A. Optical Properties of Intact Leaves for Estimating Chlorophyll Concentration. J. Environ. Qual. 2002, 31, 1424.

152. Jacquemoud, S.; Baret, F. PROSPECT: A model of leaf optical properties spectra. Remote Sens. Environ. 1990, 34, 75–91.

153. Jacquemoud, S.; Ustin, S.L. Leaf optical properties: A State of the art. In Proceedings of the 8th International Symposium of Physical Measurements & Signatures in Remote Sensing—CNES, Aussois, France, 8–12 January 2001.

154. Jacquemoud, S.; Ustin, S. Leaf Optical Properties; Cambridge University Press: Cambridge, UK, 2019.

155. Yao, X.; Zhu, Y.; Tian, Y.; Feng, W.; Cao, W. Exploring hyperspectral bands and estimation indices for leaf nitrogen accumulation in wheat. Appl. Earth. Obs. Geoinf. 2010, 12, 89–100.

156. Stellacci, A.M.; Castrignanò, A.; Troccoli, A.; Basso, B.; Buttafuoco, G. Selecting optimal hyperspectral bands to discriminate nitrogen status in durum wheat: A comparison of statistical approaches. Environ. Monit. Assess. 2016, 188, 1–15.

157. Thompson, L.J.; Puntel, L.A. Transforming Unmanned Aerial Vehicle (UAV) and Multispectral Sensor into a Practical Decision Support System for Precision Nitrogen Management in Corn. Remote Sens. 2020, 12, 1597.

158. Devadas, R.; Lamb, D.W.; Simpfendorfer, S.; Backhouse, D. Evaluating ten spectral vegetation indices for identifying rust infection in individual wheat leaves. Precis. Agric. 2008, 10, 459–470.

159. Zhao, Y.-R.; Li, X.; Yu, K.-Q.; Cheng, F.; He, Y. Hyperspectral Imaging for Determining Pigment Contents in Cucumber Leaves in Response to Angular Leaf Spot Disease. Sci. Rep. 2016, 6, 27790.
160. He, R.; Li, H.; Qiao, X.; Jiang, J. Using wavelet analysis of hyperspectral remote-sensing data to estimate canopy chlorophyll content of winter wheat under stripe rust stress. Int. J. Remote Sens. 2018, 39, 4059–4076.
161. Gao, Z.; Khot, L.R.; Naidu, R.A.; Zhang, Q. Early detection of grapevine leafroll disease in a red-berried wine grape cultivar using hyperspectral imaging. Comput. Electron. Agric. 2020, 179, 105807.
162. Calderón, R.; Navas-Cortés, J.; Zarco-Tejada, P. Early Detection and Quantification of Verticillium Wilt in Olive Using Hyperspectral and Thermal Imagery over Large Areas. Remote Sens. 2015, 7, 5584–5610.
163. Zarco-Tejada, P.J.; Camino, C.; Beck, P.S.A.; Calderon, R.; Hornero, A.; Hernández-Clemente, R.; Kattenborn, T.; Montes-Borrego, M.; Susca, L.; Morelli, M.; et al. Previsual symptoms of Xylella fastidiosa infection revealed in spectral plant-trait alterations. Nat. Plants 2018, 4, 432–439.
164. Zhao, Y.; Yu, K.; Feng, C.; Cen, H.; He, Y. Early Detection of Aphid (Myzus persicae) Infestation on Chinese Cabbage by Hyperspectral Imaging and Feature Extraction. Trans. ASABE 2017, 60, 1045–1051.
165. Pandey, P.; Ge, Y.; Stoerger, V.; Schnable, J.C. High Throughput In vivo Analysis of Plant Leaf Chemical Properties Using Hyperspectral Imaging. Front. Plant Sci. 2017, 8, 1348.
166. Zhou, W.; Zhang, J.; Zou, M.; Liu, X.; Du, X.; Wang, Q.; Liu, Y.; Liu, Y.; Li, J. Prediction of cadmium concentration in brown rice before harvest by hyperspectral remote sensing. Environ. Sci. Pollut. Res. 2018, 26, 1848–1856.
167. Ge, Y.; Atefi, A.; Zhang, H.; Miao, C.; Ramamurthy, R.K.; Sigmon, B.; Yang, J.; Schnable, J.C. High-throughput analysis of leaf physiological and chemical traits with VIS–NIR–SWIR spectroscopy: A case study with a maize diversity panel. Plant Methods 2019, 15, 66.
168. Hu, N.; Li, W.; Du, C.; Zhang, Z.; Gao, Y.; Sun, Z.; Yang, L.; Yu, K.; Zhang, Y.; Wang, Z. Predicting micronutrients of wheat using hyperspectral imaging. Food Chem. 2021, 343, 128473.
169. Fuentes, S.; Tongson, E.; Unnithan, R.R.; Gonzalez Viejo, C. Early Detection of Aphid Infestation and Insect-Plant Interaction Assessment in Wheat Using a Low-Cost Electronic Nose (E-Nose), Near-Infrared Spectroscopy and Machine Learning Modeling. Sensors 2021, 21, 5948.
170. Fang, Y.; Ramasamy, R.P. Current and prospective methods for plant disease detection. Biosensors 2015, 5, 537–561.
171. Müller, C.; Hosgood, B.; Andreoli, G. Physical mechanisms in hyperspectral BRDF data of grass and watercress. Remote Sens. Environ. 1998, 66, 222–233.
172. Ferwerda, J.G.; Skidmore, A.K.; Mutanga, O. Nitrogen detection with hyperspectral normalized ratio indices across multiple plant species. Int. J. Remote Sens. 2005, 26, 4083–4095.
173. López-Higuera, J.M. Sensing Using Light: A Key Area of Sensors. Sensors 2021, 21, 6562.